

# Details on an Annular Field Reversed Configuration Plasma Device for Spacecraft Propulsion

IEPC-2005-171

David Kirtley<sup>\*</sup>, Daniel L. Brown<sup>‡</sup>, Alec D. Gallimore<sup>§</sup>  
*University of Michigan, Ann Arbor, MI 48109*

An annular field reversed configuration (AFRC) plasma thruster concept is being developed by AFRL and the University of Michigan. This concept is derived from the coaxial slow source FRC fusion reactor concept developed at the University of Washington and has been re-tooled for space propulsion applications. A scaling energy model, commercial magnetic field model, and a proof-of-concept experiment have been completed. In addition, a complete suite of magnetic diagnostics as well as photometric and internal plasma measurements have been constructed. Results of initial tests and operation are presented, showing plasma compression, heating, and reversal.

## Nomenclature

$\beta$	=	The ratio of magnetic to particle pressures
$B_p$	=	AFRC magnetic field, measured at the exterior coil surface
$e$	=	Electron charge
$k$	=	Boltzmann's constant, $1.38 \times 10^{-23}$ J/K
$\lambda_D$	=	Debye length, cm or mm
$I$	=	Probe collected current, mA
$I_{e, \text{sat}}$	=	Electron saturation current, A
$I_{\text{ion, sat}}$	=	Ion saturation current, A
$m_e$	=	Electron mass, $9.1094 \times 10^{-31}$ kg
$n_e$	=	Plasma electron density, $\text{m}^{-3}$
$\delta$	=	Sheath thickness, cm
$r$	=	Probe electrode radius, m
$\tau$	=	Characteristic plasma resonance time, $\mu\text{s}$
$Te$	=	Maxwellian plasma electron temperature, eV
$V_{\text{bp}}$	=	Magnetic probe voltage, relative to diagnostic earth ground (V)
$V_c$	=	Discharge coil voltage, relative to capacitor return (kV)
$V_{\text{rp}}$	=	Rogoski coil voltage, relative to diagnostic earth ground (V)

## I. Introduction

Field Reversed Configuration (FRC) plasma devices have an interesting development history. These plasma devices create a relatively high-density, high  $\beta$ , high efficiency inductively coupled plasma that has many potential applications. FRCs in equilibrium have been studied extensively for fusion energy generation, while FRCs in translation have potential for devices ranging from space propulsion to tokamak refueling. In particular, the Air Force Research Laboratory is interested in utilizing an FRC plasma as a propulsion concept. Currently, there is a basic scientific research program underway to examine FRC plasmas and their use as a space propulsion concept.

---

<sup>\*</sup>Graduate Student, Aerospace Engineering, dkirtley@umich.edu.

<sup>‡</sup>Graduate Student, Aerospace Engineering, danluc@umich.edu.

<sup>§</sup> Professor and Laboratory Director, Aerospace Engineering, Associate Dean, Horace H. Rackham School of Graduate Studies, alec.gallimore@umich.edu.

## II. FRC Technology Physics

### A. FRC Physics Overview

In terms of modern FRC physics there are several subjects of interest. First, some general scaling laws of modern (1980+) FRC experiments and a general operational timeline are as follows:

- Diameters 15-90 cm
- $B_p$  1-13 kGauss
- $\beta$  0.5-1
- $n$  ( $\text{cm}^{-3}$ )  $10^{14}$  -  $10^{17}$
- $\tau$  50-500  $\mu\text{s}$

#### Translating FRC Formation

1. Fill coil with gas
2. Fill coil with low level flux
3. Pre-Ionize to trap and freeze plasma to field lines
4. Force field reversal to tear and internally reconnect field lines
5. Fully formed self-consistent FRC at this point
6. Continue pulse to radially compress, or destabilize to translate axially

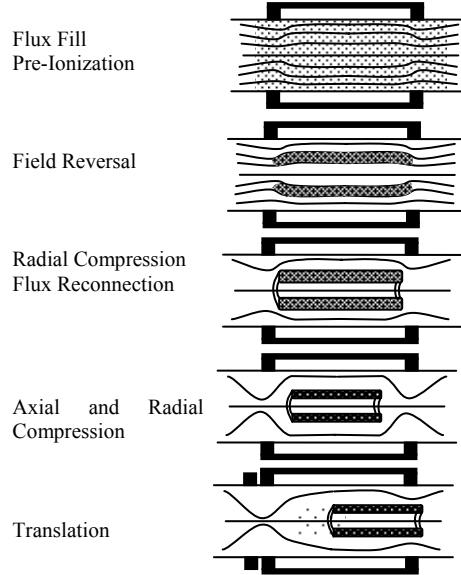


**Fig 1. Formation Sequence and Geometry**

At the exit of the FRC reactor is a compressed, relatively non-diffuse neutral toroidal plasma with a self-consistent magnetic field and large poloidal currents (relative to the toroidal plasma currents). It has been noted that forming efficient FRCs is a very empirical process of electrical circuit characteristic development; however, once a valid discharge scheme (and pre-ionization method) has been developed these reactors are very robust and repeatable<sup>1,2</sup>.

### B. Coaxial FRC Physics

Traditional FRCs have demonstrated high-velocity translation and high-efficiency compression. However, they also have some inherent disadvantages, namely high voltages (20-200 kV) and fast discharge times leading to complicated propellant feed and switching. A possible solution to these issues is the Coaxial Slow Source FRC concept (CSS) developed at the University of Washington by Vlases, Brooks, and Pierce for deuterium fusion<sup>3,4</sup>. This concept is based off of several annular, slow formation, so-called AFRC concepts developed previously<sup>5</sup>. The CSS concept has demonstrated FRC formation and translation (in excess of 10,000 sec Isp with deuterium) at coil voltages of less than 100 volts and discharge times  $> 250 \mu\text{s}$ . The CSS has approximately 100-2000V discharge voltages, 20-60 mTorr propellant pressures, and 100-500  $\mu\text{s}$  discharge times. They successfully demonstrated results similar to traditional FRC concepts (LSX<sup>6</sup> etc.), however the temperatures were insufficient for fusion, and there was some evidence of the rotational  $n=2$  instabilities that do not appear to be present in traditional FRCs. There was also evidence of excessive radiation losses due to the long discharge time and oxygen impurities. However, as our primary interest is FRC formation and immediate translation, these instabilities are of substantially less importance.

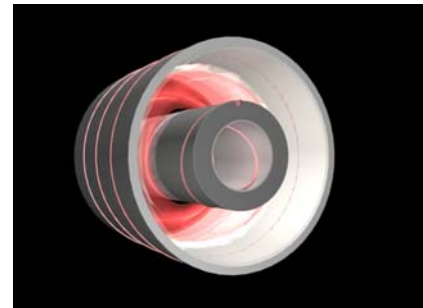


**Figure 2. 3D rendition of XOCOT**

### C. AFRL/UM XOCOT Concept

The AFRL/University of Michigan XOCOT concept geometry is based upon the general geometry of the CSS device, but is scaled to incorporate lower discharge voltages. Upgrades in capacitor technologies, switching, and general device scaling have been done with the goal of re-tooling this concept into one more suitable to space propulsion applications. Initial testing parameters are planned for 10-30 kA coil currents, 0.1-1 ms discharge times, over-all diameter of <40 cm, and >30cm length. In addition, with argon propellant and a theta-ringing RF pre-ionization discharge the XOCOT is projected to have a discharge voltage less than 1000V.

## III. AFRL FRC Technology Status Overview

### A Hardware Status

After two summers of extensive hardware development the AFRL/UM XOCOT FRC facility and experimental hardware have been completed. Figures 3-5 detail facility components that consist of the following:

- Two 1.5 m long concentric quartz tubes form the ionization region as well as the annular vacuum chamber
- 20cm (8") diffusion pump and associated vacuum hardware
- Two in-house manufactured aluminum coils (4 cm thick) are external to the chamber and form the theta coil assembly
- 18 kJ capacitor bank
- Two 30 kA+ ignitrons form the switching/transfer network
- Extensive physical, EMI, and UV shielding
- Associated high-energy safety mechanisms, including dump and bleed resistor banks

Currently installed, calibrated, and tested diagnostics include a single-pixel high speed photometer, high speed Mega Pixel (MP) single frame camera, an excluded flux array (36+ B-dot probes and several flux loops), a Rogowski coil, internal single and triple-Langmuir probes, and current and voltage monitors. Future hardware development will be targeted towards diagnostics that include high speed photography, holographic interferometry, spectroscopy, and bolometry.

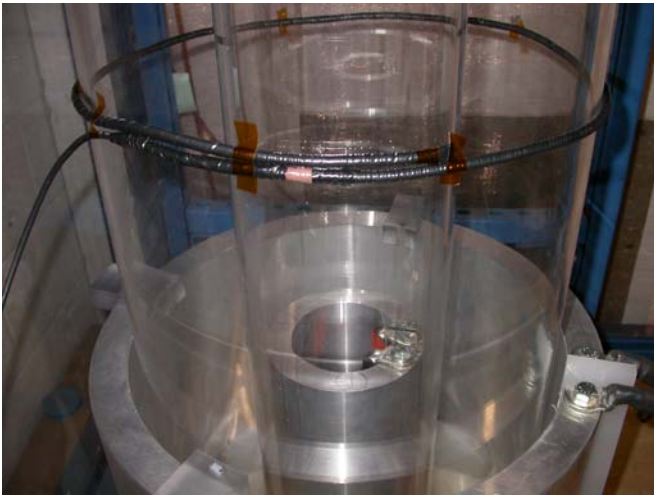


**Figure 3. Photo of the inner and outer discharge coils mounted with the annular quartz vacuum chamber. Also shown is a 40 cm Rogowski-coil and high-frequency electro-magnetic shielding**



**Figure 4. Photograph of the coils mounted in the E/M shielding cage, power supplies, and general facility setup. Note the vertical configuration of the coil/chamber assembly.**

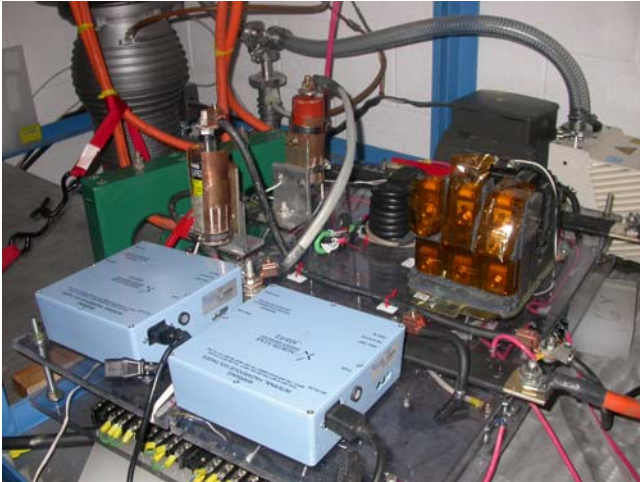


**Figure 5. Ignitron Switching Network.** This photo details the constructed type-A ignitron switch, diffusion pump, and low/high voltage switching networks. Also of note is the optical ignitron controllers from Richardson Electronics.

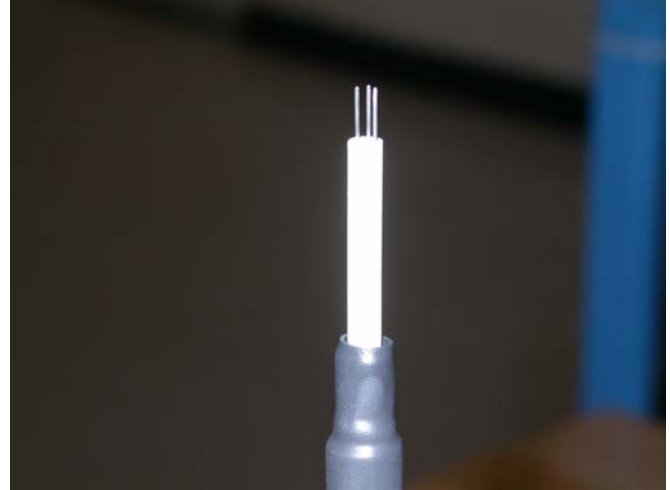


**Figure 6. Close-up photograph of the triple probe used internally with the XOCOT coils.** Probe leads are 7mm long by 0.25 mm dia, clad in a boron-nitride ceramic sheath and sealed with a vacuum-rated epoxy.

The main capacitor bank has been fully configured/constructed and tested with electrical, safety, and discharge cleanliness verified; in addition, the three main safety mechanisms, large bleed and balancing resistors, small resistance dump resistors, and capacitor grounding circuits, have been fully tested and are operational.

The primary switching, power transfer network consists of two ignitrons (mercury spark gap switches) with high-speed, high-accuracy triggering circuits. This system is fully operational with timing accuracy and turn-on times within 1  $\mu$ s and shot-to-shot repeatability demonstrated at  $\sim$ 10% (ESR, inductance).

The ignitron switching network was constructed using two 30 kA type A ignitrons and fiber-optic switches. This network can trigger the two coils independently or more interestingly, the two coils and a secondary capacitor bank for pre-ionization. The capacitor bank upgrades, safety, and electronics systems were constructed.

The primary hardware development during this construction period was geared towards diagnostics. A DICAM 2 single-color, mega-pixel single frame camera with a 10 ns resolution, and a single pixel MHz visible light photodetector were installed in several locations to optically characterize the plasma formation and heating.

Several triple probes (also used as a single Langmuir probe) were constructed from tungsten wire and alumina tubing and installed 3cm inside of the coils, centered between the two .



**Figure 7. Photograph of the 16 kJ G capacitor bank.** Not included in this photograph is the later-added RF shielding, and full kinetic shielding infrastructure.

Concomitant to hardware/facility, an extensive program of magnetic field probe (also called b-dot probes) development was underway. Several arrays of high-speed (3 mm) 3-axis probes were completed for the installed configuration between the quartz tube and discharge coil as well as between the two coils in order to map the transient magnetic field profiles of the XOCOT coils.

A Rogowski coil measures the current passing through its inner loop by sampling a circular cross-section of the magnetic flux at its periphery. Using the following equations we have designed a 1000 turn Rogowski coil with an inner diameter of 40 cm, a characteristic time response of 25 MHz, and a sensitivity of 1.5e-3 mV-s/A.

$$V_{rp} = \mu_0 n A \frac{dI_{rp}}{dt} \quad (1)$$

The goal of this Rogowski coil is to measure current of the bulk plasma translation. These, along with external magnetic field measurements should allow for a non-intrusive determination of translational velocity and kinetic energy of the AFRC plasma.

One of the primary diagnostic techniques for a field reversed plasma is an ‘excluded flux array’, an array of external magnetic probes and flux loops that can collectively measure both the shape and time evolution of the separatrix boundary of the reversed plasma<sup>7</sup>. For that purpose, as well as to map the internal magnetic field configuration of the plasma, 12 high-accuracy 2-axis B-dot probes have been constructed and calibrated for use along the exterior coils.

$$V_{bp} = n A \frac{dB_p}{dt} \quad (2)$$

In addition, 12 3-axis probes for internal magnetic field measurements have been constructed and tested using a custom-built Helmholtz coil operated between 4 and 20 kHz. Using this coil connected to a Kepco amplifier and a high-accuracy function generator a complete mapping of the linearity (and more importantly, the multiplicative constants of the probe) could be ascertained. The instrument constant for these 3 mm, 3-axis was approximately 1 mV-s/T.

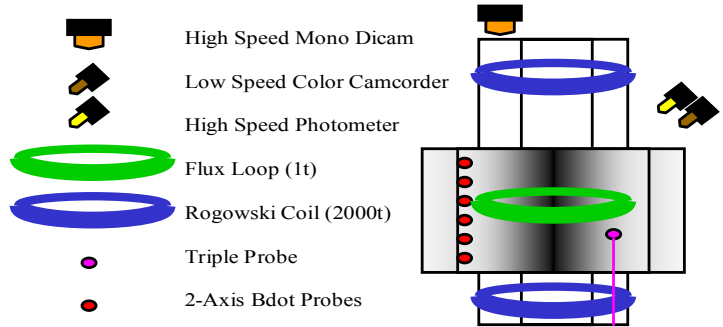


**Figure 8. Detailed probe diagram showing the locations and configuration of probes used for the initial XOCOT Testing.**

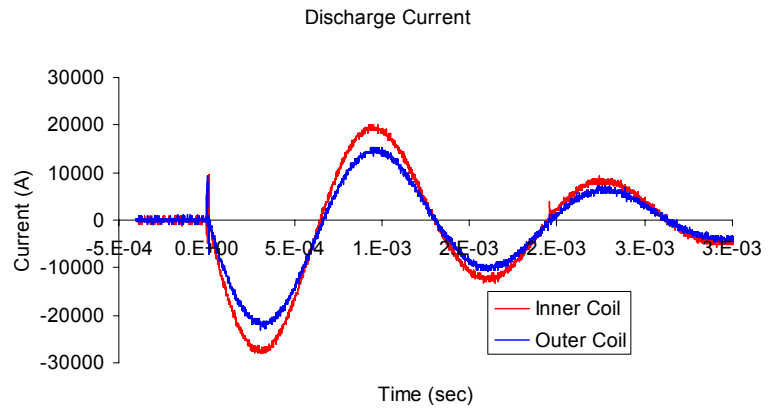
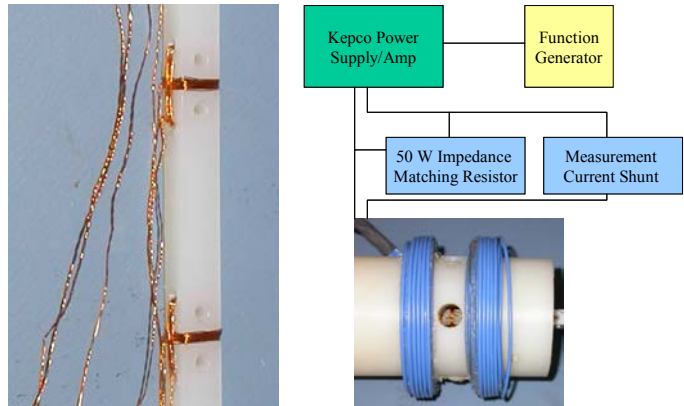


**Figure 9. A typical coaxial discharge showing the clear oscillatory and mis-matched current profiles.**



**Figures 10 and 11. A 3 mm magnetic probe and the calibration circuit used to test and validate them**

## B. Analytical/Computer Models

Currently two rudimentary computer models have been developed to support this research program. The first model, developed in order to facilitate the development of the initial concept, is a zero-dimensional energy balance model that assumes a compressed, equilibrium state (empirically based) to predict the temperature/density/energy deposition scaling as a function of XOCOT radial size. This model also takes into account the energy loss mechanisms (non-formation losses) and variations in circuit parameters, and this model shows quite clearly that at the energy levels considered, ohmic losses are a main loss mechanisms at these power levels. The model also shows that radiation losses do not become a major loss contributor until the XOCOT is operated several orders of magnitude higher discharge energy. The model also predicted (as discussed in CSS literature<sup>4</sup>) that small increases in coil size leads to <100V discharges. Secondly, by modeling the XOCOT with the COTS finite element (FEA) Magnet 3D Transient solver, the B-fields in the coils were quantified in order to validate the excluded flux array and the actual transient current density profiles for a given connection scheme. These models have clearly demonstrated that fast, large current pulses (of this type) in a large cross-sectional area are distinctly non-uniform. Future Magneto-hydrodynamic (MHD) models will enable detailed study of the internal, real-time processes occurring in the XOCOT Concept.

## IV. XOCOT Initial Tests

All data presented for the AIAA International Electric Propulsion conference were collected prior to December 2004 with more advanced data to be presented at a later date. Figures 9-14 detail typical operating characteristics and discharge current profiles. This section provides a summary and preliminary data from the XOCOT.

### A. XOCOT Initial Discharges

Extensive work has gone into an actual discharge, however, this phase of the FRC formation appears to be the most complicated of the required stages. Our review of literature confirmed our suspicion that for such a large, low-speed, low-voltage FRC, such as XOCOT, the pre-ionization discharge is the most critical phase of the discharge. As such, three discharge methods have been investigated: a DC glow discharge, a steady RF, and a high-voltage ringdown discharge.

### B. Pre-ionization discharge

The traditional theta-ringing technique of pre-ionization entails discharging a high-speed (the XOCOT current design is 2 MHz) ringing discharge at a higher voltage than the main bank (4-10 kV) but with significantly less energy than the main discharge (10's of Joules). Extensive work was done to get the pre-ionization plasma and the ignitrons to discharge fast enough with full current reversal. With only a pulsed pre-ionized discharge there was some evidence of ionization, but it was not efficient, hot, or dense enough for a proper FRC discharge. In addition, with this pre-ionization technique plasma data are lost in discharge electromagnetic noise which sponsored an extensive grounding study, isolation, E/M noise, and investigation into pulsed discharge diagnostics. In addition, noise cancellation and post processing methods were designed (filtering and reference vacuum discharge comparison).



Figure 12. Long exposure discharge photograph

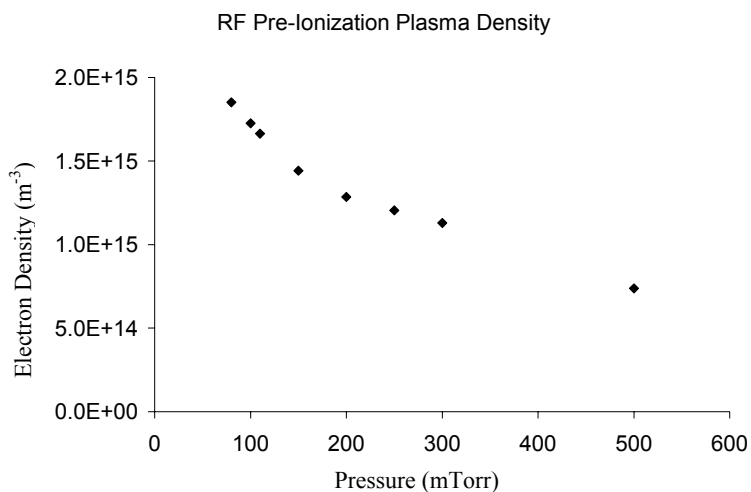
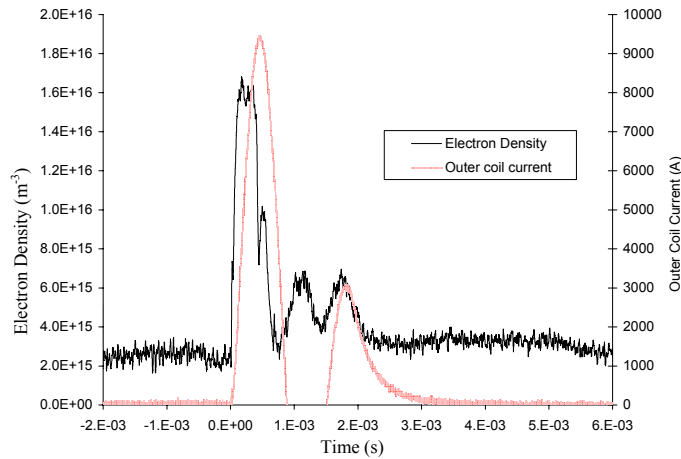
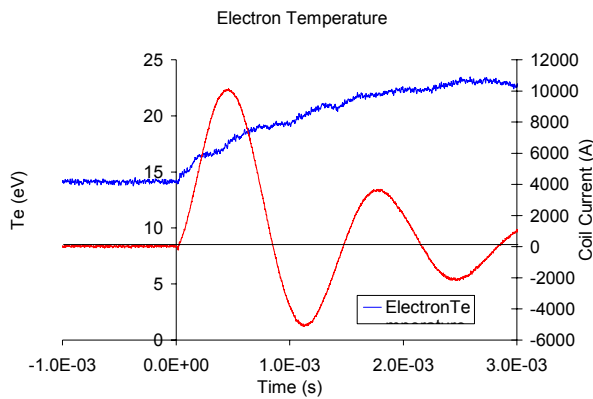


Figure 13. A typical RF pre-ionization discharge plasma number density for various fill pressures.



**Figure 14. Secondary translation coil current density profile**



**Figure 15. Typical electron temperature profile**

(within 20%) electron temperature. This acted as a strong proof of the accuracy of the triple probe measurements, during the pre-ionization region, see Fig. 13 for details.

The high-speed photometer data show several orders of magnitude increase in optical emission. The triple probe current, which corresponds linearly to electron density, follows the same general time scales and trends as the photometer data. Triple probe voltage corresponds with electron temperature and was consistently ~20 eV (Figure 15). In addition, Figure 16 presents the comparison of optical data (through a simple Boltzmann energy relation) to the internal physical probe measurements of plasma density. This comparison shows remarkable similarities in terms of general structure, and the formation and heating of the plasma during a typical discharge.

In addition, preliminary data using a secondary ‘kicker’ or translation coil (altering the magnetic profile of the mirror such to drive a translation instability) shows marked change in operation suggesting a significant decrease in plasma contained within the mirror geometry. Further work must be done to analyze plasma toroid exit velocities and profiles.

See Figures 17-18 for actual discharge photographs.

### C. Steady state RF discharge

As the previous ionization methods failed to produce efficient FRC currents in the plasma a new pre-ionization scheme was devised. Using a steady state 13.56 MHz RF supply, an efficient, stable plasma could be formed.

After the steady state RF plasma is formed, the main bank discharges the coils into it. While this method may provide poorer flux trapping, because of the geometry of the coils (and simply using two coils) there should still be field line tearing and FRC formation. As an early ionization technique, the steady-state RF approach has demonstrated easy, low voltage FRC formation, compression, and heating.

Using this method steady RF pre-ionization was created, enabling the deposition of hundreds of watts of power into the main coils. However, this method still has a low level (<1%) of ionization, while a traditional goal for the pre-ionization stage is 50%. At this stage in XOCOT development establishing a more efficient pre-ionization method is the primary research initiative. One approach that seems promising is to use the high-energy theta ringing in conjunction with a steady-state RF pre-ionization. When the main bank is discharged into this RF plasma, the applied diagnostic yields interesting results. Figures 13-15 summarize the preliminary findings.

In addition to the transient triple probe data, a relatively intensive study of the steady-state RF discharge was completed with an RF compensated single Langmuir probe<sup>8</sup> built at AFRL. We filtered the Langmuir probe for greater than 1 MHz and found repeatedly that for the same discharge pressures as the triple probe data we acquired the same plasma density and a similar

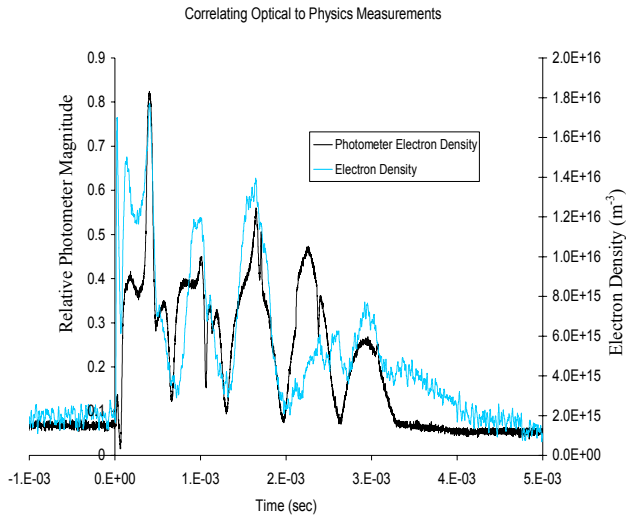


**Figure 16. Optical versus internal probe Measurements**

These preliminary data show defined plasma compression and heating during the main discharge, as well as over-all favorable local and general plasma structures. As a validation of the construction phase for this project, the data show that repeatable, EMI clean compact toroids can be produced. There are however, several questions as to the fidelity of these measurements (although the order of magnitude is correct). Further work will include improved particle collection models, resizing the probes, and perhaps better probe placement. In addition, increasing the energy (and thus plasma density) in the pre-ionization discharge will also diminish these errors.

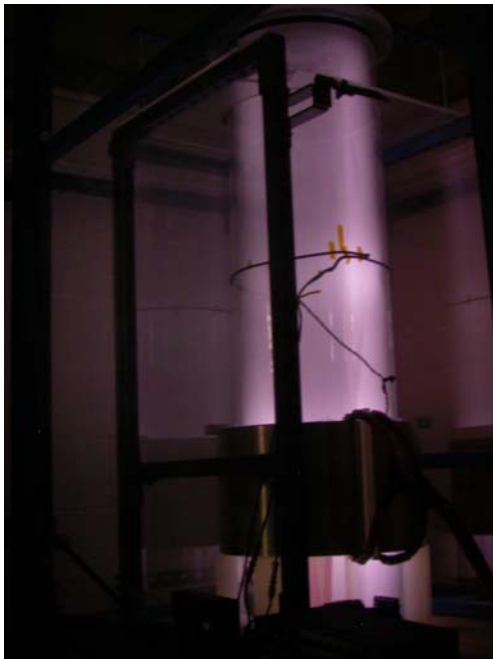


**Figure 17. RF Breakdown XOCOT coils Argon**

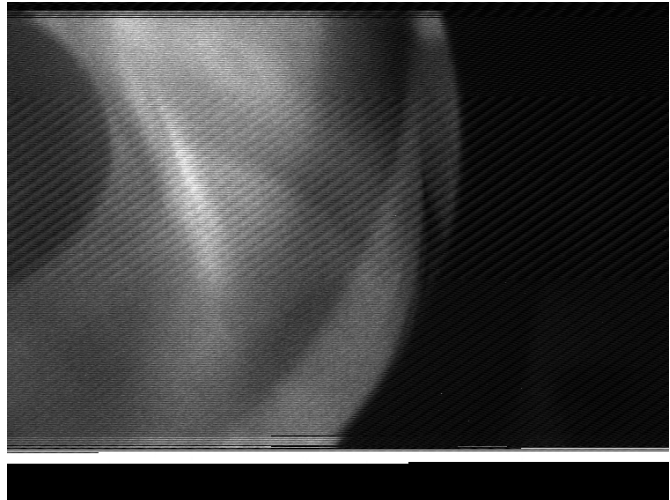


**Figure 18. Example of a high-speed (1  $\mu$ s) resolution photograph during a discharge**



## V. Conclusion

As shown above great progress has been made in the construction and testing of a FRC plasma device at the Air Force Research Laboratory. The design and construction of a facility to house the studies has been completed and preliminary testing shows that an FRC plasma has been successfully initiated, heated, and as suggested by the data, translated. Current work into characterizing the performance and detailed operation and optimization of the XOCOT is underway, in addition to general facility upgrades, EMI reduction, and data acquisition improvements. These devices hold great promise in a variety of plasma applications and warrant further study. For more information, detailed practical application, and the motivation for the study of these devices, the authors invite readers to attend the Joint Army, Navy, NASA, Air-Force Conference in December 2005.

## Acknowledgments

*I would like thank the National Science Foundation and Air Force Research Laboratories spacecraft propulsion group, specifically Dr. James M Haas, without who's funding this research would not be possible. Also, I would like to thank John Asher and Robert Gregory for their diagnostic and technical construction support.*

## References

- 
- <sup>1</sup> M. Tuszewski, Physics and Technology of Compact Toroids, Santa Fe (1985).
  - <sup>2</sup> M. Tuszewski, Rep. LA-10830-C, Los Alamos Scientific Laboratory (1986).
  - <sup>3</sup> W.F. Pierce, R.J. Maqueda et al, Nucl. Fusion **33**(117) (1993).
  - <sup>4</sup> Raman, R., Vlases, G.C., Jarboe, T.R., Nuclear Fusion **33**(1685) (1993).
  - <sup>5</sup> Jarboe T.R. Slow Formation and Sustainment of Spheromaks by a Coaxial Magnetized Plasma Source. Phys. Rev. Letters **51**(1), (1983).
  - <sup>6</sup> M. Tuszewski, Nuclear Fusion 28, 2033 (1988).
  - <sup>7</sup> Tuszewski, M., Excluded flux analysis of a field-reversed plasma. Physics of Fluids, (1981). **24**(11)
  - <sup>8</sup> Paranjpe, A.P., McVittie, J.P. A tuned Langmuir probe for measurements in rf glow discharges. J. Appl. Phys. **67**(11).

## Additional Resources

Chang Diaz, F.R, Fusion Science and Technology, 433 (2003).  
Rej, D.J., Armstrong, W.T., et al, Physics of Fluids 29, 852 (1986).  
Hagenson, R.L., Krakowski, R.A., Rep. LA-8758-MS, Los Alamos Scientific Laboratory (1981).  
Kolb, A.C., Dobbie, C.B., Phys. Rev. Lett. 3, 5 (1959).  
Steinhauer, Loren C., "Recent Advances in FRC Physics", IEEE 0-7803-2969-4 (1995).  
Syri Koelfgen, Clark Hawk, Adam Martin, et al, AIAA-2003-4992.  
Slough, J., Hoffman, A., Miller, K., STAIF 1998  
Es'Kov, A.G., Kurtmullaev, T.Kh., et al, Plasma Phys. and Nuclear Fusion 2, 187 (1979).  
Steinhauer, L.C., Milroy, R.D., Phys. Fluids 28, 888 (1985).  
Belikov, V.V., Goloviznin, V.M., et al., Plasma Phys. and Controlled Nuclear Fusion 2, 343  
Vlases. G.C. Rowe, D.S., Fusion Tech. 9, 116 (1986).  
M. Tuszewski, et al., Phys. Fluids B 3, 2856 (1991).  
J.T. Slough and A.L. Hoffman, Phys.Fluids B 5, 4366 (1993).  
Lehnert, B., Fusion Tech. 16, 7, 1989.  
Durance, G., Hogg, G.R., Tendys, J., et al, Plasma Phys. and Nuclear Fusion 29, 227 (1987).